Mode-coupling theoretical analysis of transport and relaxation properties of liquid dimethylimidazolium chloride

T. Yamaguchi[a] and S. Koda
Department of Molecular Design and Engineering, Graduate School of Engineering, Nagoya University, Furo-cho B2-3(611), Chikusa, Nagoya, Aichi 464-8603, Japan

(Received 1 December 2009; accepted 14 February 2010; published online 15 March 2010)

The mode-coupling theory for molecular liquids based on the interaction-site model is applied to a representative molecular ionic liquid, dimethylimidazolium chloride, and dynamic properties such as shear viscosity, self-diffusion coefficients, reorientational relaxation time, electric conductivity, and dielectric relaxation spectrum are analyzed. Molecular dynamics (MD) simulation is also performed on the same system for comparison. The theory captures the characteristics of the dynamics of the ionic liquid qualitatively, although theoretical relaxation times are several times larger than those from the MD simulation. Large relaxations are found in the 100 MHz region in the dispersion of the shear viscosity and the dielectric relaxation, in harmony with various experiments. The relaxations of the self-diffusion coefficients are also found in the same frequency region. The dielectric relaxation spectrum is divided into the contributions of the translational and reorientational modes, and it is demonstrated that the relaxation in the 100 MHz region mainly stems from the translational modes. The zero-frequency electric conductivity is close to the value predicted by the Nernst–Einstein equation in both MD simulation and theoretical calculation. However, the frequency dependence of the electric conductivity is different from those of self-diffusion coefficients in that the former is smaller than the latter in the gigahertz-terahertz region, which is compensated by the smaller dispersion of the former in the 100 MHz region. The analysis of the theoretical calculation shows that the difference in their frequency dependence is due to the different contribution of the short- and long-range liquid structures. © *2010 American Institute of Physics*. [doi:10.1063/1.3354117]

I. INTRODUCTION

The room-temperature ionic liquid is the molten salt whose melting temperature is below or close to the ambient temperature. It usually contains organic cation or anion as its component, and we can design the ionic liquid by tailoring the organic ions or changing the combination of ions. It can dissolve many organic molecules as well as inorganic ionic species, and it is expected to be a novel reaction media that can replace conventional organic solvents. Many researchers are thus attracted by ionic liquids at present, and there are a lot of studies on their static and dynamic properties.[1]

One of the promising applications of ionic liquids is that to the electrolyte of electrochemical devices such as lithium secondary battery and supercapacitor. Contrary to conventional organic solvents, ionic liquid possesses ionic conductivity by itself because it is composed of ions. In addition, some ionic liquids show wide electrochemical window that is suitable for high-energy electrochemical devices.

Transport properties such as electric conductivity, shear viscosity, and self- diffusion coefficients are important quantities for the applications of ionic liquids described above. Therefore, these transport properties have been measured from the beginning of the study on ionic liquids, and their experimental data have been accumulated.

The transport properties of ionic liquids have also been a target of molecular dynamics (MD) simulations. However, there are many problems in the application of MD simulation to the transport properties of ionic liquids. One of the largest difficulties is the slow structural relaxation intrinsic to many ionic liquids. Since transport coefficients are given in MD simulation by the integrals of time correlation functions over the whole time or the long-time limiting behavior of the time correlation functions, the existence of the slow structural relaxation requires the calculation of time correlation functions over long time, which then leads to the long simulation runs and poor statistics. The problem of poor statistics becomes even worse for collective properties such as electric conductivity and shear viscosity in spite of their importance in practical applications of ionic liquids. Even if these transport properties can be determined by long MD simulation and the agreement with experimental values is attained, it is much more difficult to analyze the slow dynamics of ionic liquid in order to unravel the relationship between the intermolecular interactions between ions and transport coefficients.

In this work, we apply the mode-coupling theory to an ionic liquid in order to investigate the transport coefficient and relaxation spectra. The mode-coupling theory is the theory on the dynamics of liquids that can calculate various dynamic properties from the information on static structures. It was originally developed for simple liquids, and it has been applied to analyze the dynamics of monoatomic

[a]Author to whom correspondence should be addressed. Electronic mail: tyama@nuce.nagoya-u.ac.jp.

liquids.[2–4] However, Chong and co-workers[5,6] extended the mode-coupling theory to molecular liquids based on the interaction-site model about a decade ago, which enabled us to study the molecular systems of chemical interests such as high-pressure water[7] and aqueous solutions.[8–10] In addition, the mode-coupling theory for atomic liquids was extended also to atomic mixtures,[11,12] and successfully applied to the dynamics of inorganic molten salts.[13,14]

The mode-coupling theory is superior to MD simulation in the following two points. First, it can evaluate the long-time dynamics without statistical errors that is inevitably involved in MD simulation. Second, it can analyze the origin of the long-time dynamics in terms of the analytical expression of the memory function. On the other hand, it suffers from the errors due to the approximation to derive the closed expression for the memory function. In this work, the results of the mode-coupling theory is compared with MD simulation to test the ability of the former to describe the transport properties and slow dynamics of ionic liquids, and the origin of the slow relaxation of ionic liquids is discussed in terms of the theoretical calculation.

II. NUMERICAL METHODS

A. Model system

The model system employed in this work is dimethylimidazolium chloride, hereafter described as [mmim]Cl, which is a representative model of ionic liquids used in various simulation and theoretical studies.[15–23] Since mmim cation does not possess the intramolecular degree of freedom associated with an alkyl chain, we can treat it as a rigid molecule. The potential parameters determined by Hanke and co-workers[15] for the united atom model of mmim cation are employed, and the intramolecular geometry of mmim cation is determined as is proposed by Lopes and co-workers.[24] In the united atom model of Hanke and co-workers, the methyl groups of the mmim cation are regarded as united atoms, and other hydrogen atoms are handled explicitly.

The temperature of the system is 400 K, and the number density of each ion is 0.005 29 molecule/Å^3. The latter value is reported by Hanke and co-workers as the number density at 400 K and ambient pressure.[15]

B. MD simulation

An MD simulation run is performed under the microcanonical condition. The shape of the simulation cell is cubic, and the periodic boundary condition is employed. The number of ion pairs in the simulation cell is 250. The length of the equilibration run is 2.5 ns, and the simulation run of 25 ns length is performed subsequently in order to calculate the correlation functions. The reorientational degree of freedom is described by quartanion, and the symplectic algorithm proposed by Miller and co-workers[25] is employed for the integration of the equation of motion with the time step of 5 fs. The long-range Coulombic interaction is treated with the Ewald method. The temperature of the system is controlled by scaling the linear and angular velocity of the molecules during the equilibration run.

C. Static structure as the input of mode-coupling theoretical calculation

The site-site static structure factor is required as the input of the theoretical calculation based on the mode-coupling theory. Although the static structure factor can be evaluated from the intermolecular interaction analytically by reference interaction-site model (RISM) integral equation theory,[19,20,22,23] we calculate the static structure factor from the site-site radial distribution function obtained in our MD simulation in order to exclude the additional errors through the static structure. Since the radial distribution functions from the MD simulation are limited to the half-length of the simulation cell, we extend them to infinite distance with the help of the RISM theory in the following way.

The RISM theory requires a closure equation, which is a local relationship between the radial distribution functions $[g_{\alpha\gamma}(r)]$, direct correlation functions $[c_{\alpha\gamma}(r)]$, and site-site interaction potential $[u_{\alpha\gamma}(r)]$, where α and γ are used for indices for interaction sites. One of the representative closure is the Kovalenko–Hirata (KH) one, which is given by[26]

$$g_{\mathrm{KH},\alpha\gamma}(r) = \begin{cases} 1 + \xi_{\alpha\gamma}(r) & (\xi_{\alpha\gamma}(r) > 0) \\ \exp[\xi_{\alpha\gamma}(r)] & (\xi_{\alpha\gamma}(r) < 0), \end{cases} \tag{1}$$

$$\xi_{\alpha\gamma}(r) \equiv h_{\alpha\gamma}(r) - c_{\alpha\gamma}(r) - \frac{u_{\alpha\gamma}(r)}{k_B T}, \tag{2}$$

where $h_{\alpha\gamma}(r) \equiv g_{\alpha\gamma}(r) - 1$ denotes the total correlation function, and k_B and T stand for the Boltzmann constant and absolute temperature, respectively.

In this work, the closure equation is modified as

$$g_{\alpha\gamma}(r) = \phi(r) g_{\mathrm{MD},\alpha\gamma}(r) + [1 - \phi(r)] g_{\mathrm{KH},\alpha\gamma}(r), \tag{3}$$

where $g_{\mathrm{MD},\alpha\gamma}(r)$ stands for the radial distribution function obtained by the MD simulation. The switching function $\phi(r)$ is determined so that $g_{\alpha\gamma}(r) = g_{\mathrm{MD},\alpha\gamma}(r)$ in the short-range region, whereas the long-range behavior is given by the KH closure. The explicit functional form of $\phi(r)$ employed in this work is given by

$$\phi(r) = \begin{cases} \frac{1}{2}\left[1 - \sin\left(\frac{\pi(r - r_0)}{2\Delta r}\right)\right] & (|r - r_0| < \Delta r) \\ 1 - \theta(r - r_0) & (|r - r_0| > \Delta r). \end{cases} \tag{4}$$

The values of r_0 and Δr are 5 and 2 Å, respectively.

The combination with the integral equation theory is a traditional way to extend the radial distribution function obtained by MD simulation of simple liquids,[27] and we consider our method described above is its natural extension to molecular liquids.

D. Mode-coupling theoretical calculation

The mode-coupling theory is the theory that deals with the time dependence of the site-site dynamic structure factor and its self-part, denoted as $\mathbf{F}(k,t)$ and $\mathbf{F}^s(k,t)$, respectively, which denote the matrices whose suffices are indices for interaction sites. The definitions of $\mathbf{F}(k,t)$ and $\mathbf{F}^s(k,t)$ are given by

$$F_{\alpha\gamma}(k,t) \equiv \frac{1}{V}\langle \rho_\alpha^*(\mathbf{k},t=0)\rho_\gamma(\mathbf{k},t)\rangle, \tag{5}$$

$$F_{\alpha\gamma}^s(k,t) \equiv \langle \rho_\alpha^{s*}(\mathbf{k},t=0)\rho_\gamma^s(\mathbf{k},t)\rangle, \tag{6}$$

where $\rho_\alpha(\mathbf{k},t)$ and $\rho_\alpha^s(\mathbf{k},t)$ stand for the density field of the whole α site and those of the α site within a tagged molecule, respectively. The time dependence of these correlation functions is given by the generalized Langevin equation described as[28]

$$\ddot{\mathbf{F}}(k,t) + k^2\mathbf{J}(k)\cdot\boldsymbol{\chi}^{-1}(k)\cdot\mathbf{F}(k,t) + \int_0^t d\tau\mathbf{K}(k,t-\tau)\cdot\dot{\mathbf{F}}(k,\tau) = \mathbf{0}, \tag{7}$$

$$\ddot{\mathbf{F}}^s(k,t) + k^2\mathbf{J}^s(k)\cdot\boldsymbol{\omega}^{-1}(k)\cdot\mathbf{F}^s(k,t) + \int_0^t d\tau\mathbf{K}^s(k,t-\tau)\cdot\dot{\mathbf{F}}^s(k,\tau) = \mathbf{0}. \tag{8}$$

Here, the static correlation functions that appear in the equation above are defined as

$$\boldsymbol{\chi}(k) \equiv \mathbf{F}(k,t=0), \tag{9}$$

$$\boldsymbol{\omega}(k) \equiv \mathbf{F}^s(k,t=0), \tag{10}$$

$$\mathbf{J}(k) \equiv -\frac{1}{k^2}\ddot{\mathbf{F}}(k,t=0), \tag{11}$$

$$\mathbf{J}^s(k) \equiv -\frac{1}{k^2}\ddot{\mathbf{F}}^s(k,t=0). \tag{12}$$

The memory functions, denoted as $\mathbf{K}(k,t)$ and $\mathbf{K}^s(k,t)$ for collective and self-dynamics, respectively, stand for the frictional force on the dynamic structure factor and its self-part, respectively. The mode-coupling theory approximates the memory function as the bilinear product of the dynamic structure factor as[6]

$$[\mathbf{J}^{-1}(k)\mathbf{K}_{MCT}(k,t)]_{\alpha\gamma} = \frac{1}{8\pi^3}\int d\mathbf{q}\{q_z^2[\mathbf{c}(q)\cdot\mathbf{F}(q,t)\cdot\mathbf{c}(q)]_{\alpha\gamma}\mathbf{F}^{\alpha\gamma}(|\mathbf{k}-\mathbf{q}|,t) + q_z(k-q_z)[\mathbf{c}(q)\cdot\mathbf{F}(q,t)]_{\alpha\gamma}|\mathbf{F}(|\mathbf{k}-\mathbf{q}|,t)\cdot\mathbf{c}(|\mathbf{k}-\mathbf{q}\,)|_{\alpha\gamma}\}, \tag{13}$$

$$[\mathbf{J}^{s,-1}(k)\mathbf{K}_{MCT}^s(k,t)]_{\alpha\gamma} = \frac{1}{8\pi^3}\int d\mathbf{q}q_z^2[\mathbf{c}(q)\cdot\mathbf{F}(q,t)\cdot\mathbf{c}(q)]_{\alpha\gamma}\mathbf{F}^{s,\alpha\gamma}(|\mathbf{k}-\mathbf{q}|,t), \tag{14}$$

where z-axis is defined to be parallel to the direction of $\mathbf{k}$-vector. The correction of the memory function proposed by Yamaguchi and Hirata[29] to include the interaxial coupling is not employed in this work for simplicity.

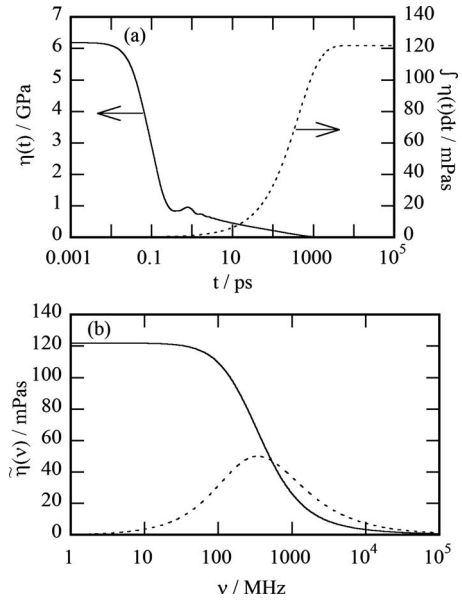

FIG. 1. The time- or frequency-dependent shear viscosity calculated by the mode-coupling theoretical calculation are exhibited. In panel (a), the time-dependent shear viscosity $\eta(t)$ and its running integral are plotted as the solid and dotted curves, respectively. In panel (b), the real and imaginary parts of the frequency-dependent shear viscosity are shown as the solid and dotted curves, respectively.

III. RESULTS AND DISCUSSIONS

A. Shear viscosity

The zero-frequency shear viscosity, denoted as η_0, is related by the Kubo–Green formula to the time-integration of the time correlation function of the shear stress as[3,4]

$$\eta_0 = \int_0^\infty dt\,\eta(t), \tag{15}$$

$$\eta(t) \equiv \frac{V}{k_BT}\langle\sigma_{xz}(0)\sigma_{xz}(t)\rangle, \tag{16}$$

where $\boldsymbol{\sigma}(t)$ stands for the stress tensor.

In the mode-coupling theory employed in this work, the expression for the time- dependent shear viscosity $\eta(t)$ is derived as the long-wavelength limit of the memory function for the transverse current as

$$\eta(t) = \frac{k_BT}{60\pi^2}\int_0^\infty dk k^4\,\mathrm{Tr}\left[\left\{\frac{d\mathbf{c}(k)}{dk}\cdot\mathbf{F}(k,t)\right\}^2\right]. \tag{17}$$

Figure 1(a) shows the time-dependent shear viscosity $\eta(t)$ and its running integral calculated by the mode-coupling theory as the function of time. The relaxation of the shear stress is clearly observed in 100 ps region, and the zero-frequency shear viscosity is determined by this slow relaxation. There are many MD simulation studies on the shear viscosity of ionic liquids, and the relaxation of the shear stress in the time scale of 100 ps is observed also in MD simulations.[18,30,31] The theoretical value of η_0 is 122 mPa s. Bhargava and Balasubramanian[18] performed the MD simulation with a potential model different from ours, and they obtained 48 mPa s as the value of the shear viscosity at 425 K, which is about half of our theoretical value. The

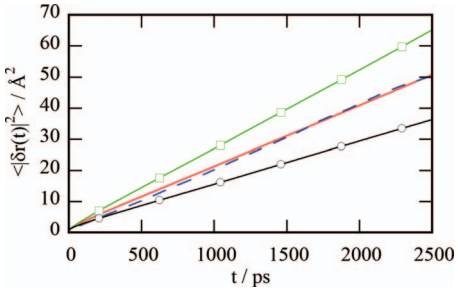

FIG. 2. The mean-square displacements $\langle|\delta r(t)|^2\rangle$ obtained by the MD simulation are plotted as the function of time. The mean-square displacements of cation and anion are plotted as the green solid curves with squares and the black solid curves with circles, respectively. The red solid curve denotes their average and the mean-square displacement of the charge center, defined by Eq. (30), is shown as the blue dashed curve.

difference is probably due to the approximation in the theoretical calculation because the mode-coupling theory tends to underestimate the molecular mobility as will be shown later.

The slow relaxation in the time correlation function associated with the transport coefficient is usually observed in experiments as the frequency dependence of the transport coefficient. The frequency-dependent complex shear viscosity is given by

$$\tilde{\eta}(\nu) = \eta'(\nu) - i\eta''(\nu) = \int_0^\infty dt e^{-2\pi i\nu t}\eta(t). \tag{18}$$

The frequency-dependent shear viscosity is exhibited in Fig. 1(b). A large relaxation is found in the 100 MHz region. Experimentally, Makino and co-workers measured the ultrasonic absorption coefficients of some ionic liquids at three different frequencies between 10 and 100 MHz and found the relaxation in the longitudinal viscosity in this frequency region.[32] Since the longitudinal viscosity is closely related to the shear viscosity, one can expect similar relaxation also in the shear viscosity. The existence of the ultrasonic relaxation in 100 MHz region is also reported by Fukuda and co-workers[33] as the frequency-dependence of the sound velocity. In addition, our preliminary experimental result shows that the shear viscosities of some ionic liquid depend on frequency between 5 and 200 MHz at the ambient condition.[34]

B. Self-diffusion and single-molecular reorientational relaxation

Figure 2 shows the mean-square displacements of the centers-of-mass of ions obtained by the MD simulation as the function of time. Linear relationship is found at $t > 500$ ps, and the diffusion coefficients are determined from the slope between 1.0 and 2.5 ns as $D_+ = 4.23 \times 10^{-11}$ m^2/s and $D_- = 2.30 \times 10^{-11}$ m^2/s, where D_+ and D_- stand for the diffusion coefficients of cation and anion, respectively. These values are several times smaller than the corresponding values reported by Hanke and co-workers,[15] $D_+ = 11 \times 10^{-11}$ m^2/s and $D_- = 8 \times 10^{-11}$ m^2/s. We consider that the reason for the difference between their values and ours is because the time length of the mean-square displacement was short in their simulation. The mean-square displacement of our MD simulation between 0 and 20 ps is exhibited in Fig. 3(a), which agrees well with the corresponding functions demonstrated in Fig. 4 of Ref. 15. However, as is demonstrated in Fig. 3(b), the slopes of the mean-square displacement become smaller with an increase in time in the 100 ps region. Therefore, the diffusion coefficient determined from the slope at shorter time must be larger than that from the slope at longer times. In our MD simulation, because the diffusion coefficients determined from the slope between 0.5 and 1.0 ns agree with that from the slope between 1.0 and 2.5 ns within 5%, we consider that the length of our mean-square displacement is sufficiently long to determine the diffusion coefficients. The similar relaxation in the slope of mean-square displacement has been reported in previous MD simulation studies of ionic liquids.[35,36] The existence of the slow relaxation in the diffusion coefficient is in harmony with the corresponding relaxation in shear viscosity since the diffusion coefficient is often correlated with the shear viscosity.

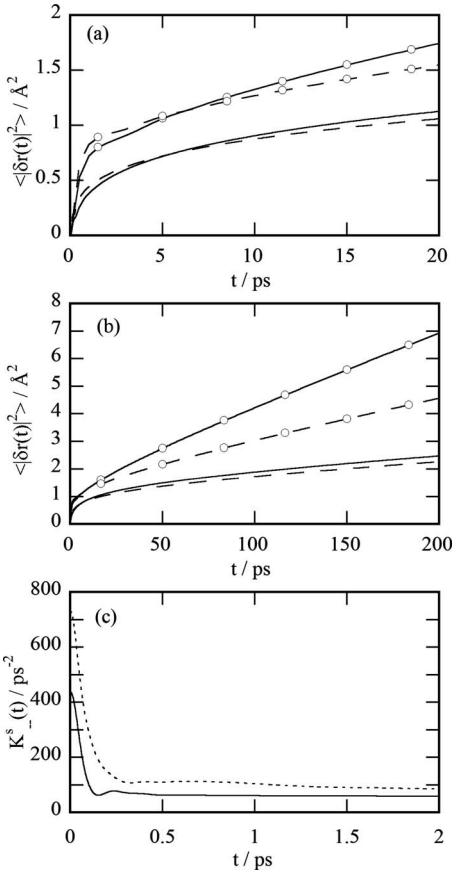

FIG. 3. The self-motions of ions from MD simulation and theoretical calculation are compared. Panels [(a) and (b)] show the mean-square displacements of ions obtained by theoretical calculation (curves without symbols) and those from MD simulation (curves with circles). The functions for cation and anion are plotted as the solid and dashed curves, respectively. In panel (c), the memory function of anion from theoretical calculation (dotted curve) are exhibited together with that from MD simulation (solid curve).

The diffusion coefficients obtained by the mode-coupling theory are $D_+ = 0.65 \times 10^{-11}$ m^2/s and $D_- = 0.63 \times 10^{-11}$ m^2/s, which is several times smaller than those of our MD simulation. Since mode-coupling theory tends to underestimate the molecular mobilities of supercooled

liquids,[37] the smaller diffusion coefficients of the mode-coupling theory are regarded as the general behavior of the mode-coupling theory.

The theoretical mean-square displacements are compared with MD simulation in Figs. 3(a) and 3(b). The theory reproduces the simulation results qualitatively in the 10 ps scale, as is demonstrated in Fig. 3(a). In particular, the slopes of the mean-square displacement agree with each other around 10 ps. Since the diffusion coefficient is determined by the slope of the mean-square displacement, it can be said that the mode-coupling theory describes the diffusive motion of ions in the 10 ps scale. On the other hand, the difference between the theory and simulation increases with an increase in time, as is shown in Fig. 3(b). Although the decrease in the slopes is observed both in theory and simulation, the magnitude of the decrease in slope is larger in the theory than in the MD simulation, which leads to the smaller diffusion coefficients in the theoretical calculation. In addition, the difference between D_+ and D_-, which stems from the long-time dynamics in MD simulation, is not described sufficiently in the theoretical calculation.

Figure 3(c) compares the memory functions for the self-diffusion of anion evaluated by the theory and MD simulation. The memory functions of the MD simulation is calculated from the velocity autocorrelation function as was performed by Yamaguchi and co-workers.[38] The theoretical memory function qualitatively resembles to that of MD simulation, although the amplitude of the former is larger than the latter. The memory function consists of fast binary part and slow relaxation, as is the case of simple liquids.[2,38] Since the relaxation of the latter is quite slow, the former contributes little to the diffusion coefficient in the long-time limit.

The rank-1 reorientational relaxation times of the vectors along C_2 axis and that connecting two nitrogen atoms, hereafter called τ_{1x} and τ_{1y}, respectively, are calculated by both mode-coupling theory and MD simulation. The reorientational relaxation times are determined as the time-integration of the normalized rank-1 reorientational correlation functions. The values of τ_{1x} and τ_{1y} are 151 and 270 ps, respectively, in our MD simulation, and 836 and 1160 ps in the mode-coupling theory. The relaxation times of the theory are several times larger than those of MD simulation, as is the case of self-diffusion coefficient. The relaxation times of our MD simulation are larger than those reported by Hanke and co-workers,[15] τ_{1x} and τ_{1y} are 88 and 145 ps, respectively. The reorientational correlation functions deviate from the exponential functional form within 100 ps, although the result is not shown for brevity. We therefore consider that the difference in the length of the calculated correlation functions is also the reason for the difference in the relaxation times.

C. Electric conductivity and dielectric relaxation

The frequency-dependent electric conductivity is related to the low-wavenumber limit of the dynamic structure factor. First, the frequency-dependent electric susceptivity, denoted as $\epsilon_{\mathrm{el}}(\nu)$, is given by[4]

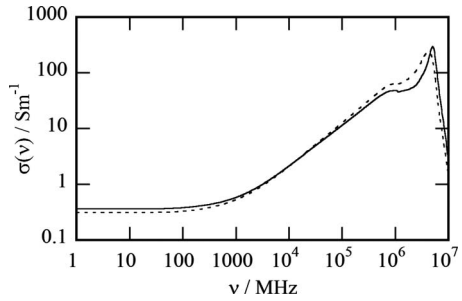

FIG. 4. The frequency-dependent electric conductivity determined by the theoretical calculation is plotted as the solid curve, and compared with the result of the frequency-dependent Nernst–Einstein relationship, Eq. (34) (dotted curve).

$$\frac{1}{\epsilon_{\mathrm{el}}(\infty)} - \frac{1}{\epsilon_{\mathrm{el}}(\nu)} = \Phi(t=0) - 2\pi\nu i \int_0^\infty dt e^{-2\pi i \nu t} \Phi(t), \quad (19)$$

$$\Phi(t) \equiv \lim_{k\to 0} \frac{1}{\epsilon_0 k_B T k^2} \sum_{\alpha\gamma} z_\alpha z_\gamma F_{\alpha\gamma}(k,t), \quad (20)$$

where ϵ_0 and z_α stand for the dielectric constant of vacuum and the partial charge on the α site, respectively. The frequency-dependent electric conductivity $\sigma(\nu)$ is then obtained as

$$\sigma(\nu) \equiv \sigma'(\nu) + i\sigma''(\nu) = 2\pi\nu\epsilon_0 i[\epsilon_{\mathrm{el}}(\nu) - 1]. \quad (21)$$

The dielectric constant at the infinite frequency $\epsilon_{\mathrm{el}}(\infty)$ is unity in our model because the electronic polarization of ions is not included.

The real-part of the electric conductivity $\sigma'(\nu)$ is plotted as the function of frequency in Fig. 4. The direct-current (dc) electric conductivity is 0.367 S/m, and the conductivity shows large dispersion above 100 MHz, as is the case of shear viscosity.

The dielectric relaxation spectrum $\epsilon(\nu)$ of conductive liquids is usually defined by subtracting the effect of dc conductivity $\sigma_0 \equiv \sigma(\nu=0)$ from $\epsilon_{\mathrm{el}}(\nu)$ as

$$\epsilon(\nu) \equiv \epsilon_{\mathrm{el}}(\nu) - \frac{\sigma_0}{2\pi\nu\epsilon_0 i} = 1 + \frac{\sigma(\nu) - \sigma_0}{2\pi\nu\epsilon_0 i}. \quad (22)$$

The dielectric relaxation spectrum calculated from the frequency-dependent conductivity is demonstrated in Fig. 5. The real and imaginary parts are plotted separately in panels (a) and (b), respectively. A large and broad relaxation is found in 100 MHz region, as has been reported in literatures for various ionic liquids.[39–42] The *static* dielectric constant, which is defined as the zero-frequency limiting value of the real part of $\epsilon(\nu)$, is 22. The experimental values of static dielectric constant measured by microwave experiments ranging from 10 to 30, and we consider that the relaxation amplitude in our theory is also in harmony with the experiments. In addition, a resonance-shaped structure is found at several terahertzs, as was observed by terahertz spectroscopy experimentally.[43]

The definition of the dielectric relaxation spectrum in Eq. (22) assumes implicitly that the translational diffusive motion of ions is Markovian, that is, the translational mobility of ions does not depend on frequency. The relaxation

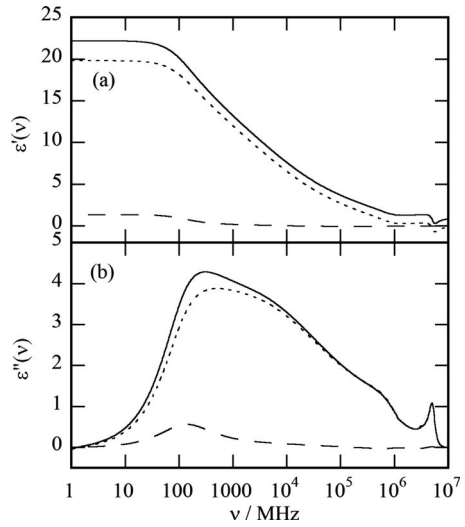

FIG. 5. The real and imaginary parts of the dielectric relaxation spectra obtained by the theoretical calculation are plotted in panels [(a) and (b)], respectively. The total relaxation spectrum (solid curves) is divided into the contributions of translational (dotted curves) and reorientational (dashed curves) modes.

observed in 100 MHz region has thus been assigned to the reorientational relaxation of cations in the analysis of experiments.[39–42] On the other hand, the shear viscosity also shows a relaxation in the same frequency region as is shown in Fig. 1. Correspondingly, the slope of the mean-square displacement of the center-of-mass of ions depends on time in the 100 ps region, which indicates that the single-molecular translational diffusion of ions is dependent on frequency in the 100 MHz region. It is therefore natural to consider that the translational mobility of ions is also frequency-dependent which leads to the contribution of the translational modes to the dielectric relaxation spectrum.

The contribution of the translational modes to the dielectric relaxation of ionic liquids was suggested by theoretical study,[44] and some MD simulations indicate that the dielectric relaxation spectrum is affected by the translational motion of ions.[45–47] In MD simulations, the relaxation due to the translational mode is faster than that due to the reorientational relaxation, and the slowest relaxation is generally ascribed to the reorientational mode. However, it is difficult for MD simulation to determine the translational part of the dielectric relaxation spectrum in the 100 MHz region, because it requires the calculation of the slow and small relaxation of the time correlation function of the collective ionic current.

The translational part of the frequency-dependent conductivity, denoted as $\sigma_T(\nu)$, is defined in terms of the response of the center-of-mass motion of ions to the applied electric field. It is also related to the low wavevector limit of the dynamic structure factor as

$$\sigma_T(\nu) = 2\pi\nu i \epsilon_0 \epsilon_{\mathrm{el}}(\nu)\left[\Phi_T(0) - 2\pi\nu i \int_0^\infty dt\, e^{-2\pi\nu t i}\Phi_T(t)\right], \tag{23}$$

$$\Phi_T(t) \equiv \lim_{k\to 0} \frac{1}{\epsilon_0 k_B T k^2} \sum_\zeta z_\zeta \sum_{\alpha\in\zeta} \frac{m_\alpha}{m_\zeta} \sum_\gamma F_{\alpha\gamma}(k,t), \tag{24}$$

although the derivation is omitted for simplicity. Here, ζ is used for the index of ionic *species*, and z_ζ and m_ζ denote the total charge and mass of the ion ζ, respectively. The translational part of the dielectric relaxation, $\epsilon_T(\nu)$ is then defined through $\sigma_T(\nu)$ as

$$\epsilon_T(\nu) \equiv \frac{\sigma_T(\nu) - \sigma_T(0)}{2\pi\nu i}. \tag{25}$$

The reorientational parts of the conductivity and dielectric relaxation spectra, denoted as $\sigma_R(\nu)$ and $\epsilon_R(\nu)$, respectively, are obtained as

$$\sigma_R(\nu) \equiv \sigma(\nu) - \sigma_T(\nu), \tag{26}$$

$$\epsilon_R(\nu) \equiv \frac{\sigma_R(\nu)}{2\pi\nu i}. \tag{27}$$

The contribution of dc conductivity does not appear in Eq. (27) because $\sigma_R(0)=0$. The dielectric relaxation spectrum is divided into the translational and reorientational parts and is demonstrated in Fig. 5. As is clearly seen, the dielectric relaxation stems from the translational mode of ions. In particular, the principal relaxation observed in 100 MHz region, which has been ascribed to the reorientational relaxation of cation, is assigned mainly to the translational mode. Although the contribution of the reorientational mode also exists in the similar frequency region, its relaxation amplitude is much smaller than that of the translational mode. In addition, the structure at several terahertzs is assigned exclusively to the translational mode. It can therefore be interpreted as the vibrational motion of ions within the cage formed by their respective counterions.

One may consider that the dominance of the translational mode in the dielectric relaxation spectrum in our calculation is because the dipole moment of the mmim cation is small due to high symmetry of mmim cation in our model. We admit that the contribution of the reorientational mode of cation will be larger if the length of one of the alkyl chains of the cation is increased. However, we consider we can safely say that the translational mode makes non-negligible contribution to the principal relaxation of $\epsilon(\nu)$ of imidazolium-based ionic liquids in general.

Although the dielectric relaxation of ionic liquid has been discussed in terms of the reorientational relaxation of cations, it possesses some properties that require special explanation in order to interpret as the reorientation of cations. First, the change in the static dielectric constant with increasing the alkyl chain length of imidazolium cation is rather small compared with the increase in the dipole moment of cations.[40,41] Second, the absolute value of the static dielectric constant of an ionic liquid is too large compared with the value estimated from the dipole moment and the number density of the cation, and one needs to assume strong positive correlation between cations in order to explain the dielectric constant by the reorientational relaxation alone.[42] Third, the dielectric relaxation times of some ionic liquids

do not agree with the values from other experiments such as nuclear magnetic resonance or depolarized light scattering.[41,48] We consider that the contribution of the translational mode to the dielectric relaxation can be a candidate to resolve these problems.

D. Cooperativity in ionic transport

Under the assumption that the diffusive motions of different ions are not correlated, the Nernst–Einstein relationship describes the dc electric conductivity in terms of the self-diffusion coefficients of ions as

$$\sigma_{\mathrm{NE},0} = \sum_{\zeta} \frac{\rho_{\zeta} z_{\zeta}^2 D_{\zeta}}{k_B T}, \tag{28}$$

where ρ_{ζ} and D_{ζ} stand for the number density and diffusion coefficient of ion ζ, respectively. The theoretical value of $\sigma_{\mathrm{NE},0}$ is 0.316 S/m, and the ratio of σ_0 to $\sigma_{\mathrm{NE},0}$, called *ionicity* in the field of ionic liquid, is 1.16 in our theoretical calculation. On the other hand, the experimental values of ionicity are usually smaller than unity, and they are discussed in terms of the formation of ion pairs.[49–52]

In order to clarify the reason of large ionicity, the electric conductivity is also calculated in our MD simulation. The electric conductivity can be evaluated in MD simulation from the slope of the mean-square displacement of the charge center, denoted as $\langle|\delta r_{\mathrm{el}}(t)|^2\rangle$, as

$$\sigma_0 = \frac{\rho e^2}{12 k_B T} \lim_{t\to\infty} \frac{d}{dt} \langle|\delta r_{\mathrm{el}}(t)|^2\rangle, \tag{29}$$

$$\langle|\delta r_{\mathrm{el}}(t)|^2\rangle \equiv \frac{1}{N_+ + N_-} \langle|\mathbf{r}_{\mathrm{el}}(t) - \mathbf{r}_{\mathrm{el}}(0)|^2\rangle, \tag{30}$$

$$\mathbf{r}_{\mathrm{el}}(t) \equiv \sum_i \frac{z_i}{e} \mathbf{r}_i(t), \tag{31}$$

where i is used for the index of ions, and $\mathbf{r}_i(t)$ stands for the center-of-mass position of ion i. N_+ and N_- mean the number of cation and anion, respectively, and ρ denotes the number density of ion pairs. Since the ionic liquid we study in this work is monovalent, the charge on ion i is $z_i = \pm e$. When the motion of different ions is not correlated, $\langle|\delta r_{\mathrm{el}}(t)|^2\rangle$ is related to the average of the mean-square displacements of individual ions as

$$\langle|\delta r_{\mathrm{el}}(t)|^2\rangle = \tfrac{1}{2}[\langle|\delta r_+(t)|^2\rangle + \langle|\delta r_-(t)|^2\rangle]. \tag{32}$$

The substitution of Eq. (32) into Eq. (29) reduces to the Nernst–Einstein relationship, Eq. (28).

The mean-square displacement of the charge center is shown in Fig. 2. The average of the mean-square displacements of cation and anion, which is the right-hand side of Eq. (32), is plotted together. They agree with each other well, which indicates that the Nernst–Einstein relationship holds approximately. From the slope between 1.0 and 2.5 ns, the electric conductivity is 1.70 S/m, and the value of ionicity is 1.06.

Since the ionicity is close to unity in both MD simulation and theory, the disagreement with experiments is ascribed to the model employed in this work, and our theoretical calculation describes the cooperativity of the ionic transport rather well. Castro and Vega[30] performed MD simulations on 1-ethyl-3-methylimidazolium chloride, and they also obtained the electric conductivity close to the prediction of Nernst–Einstein relationship.

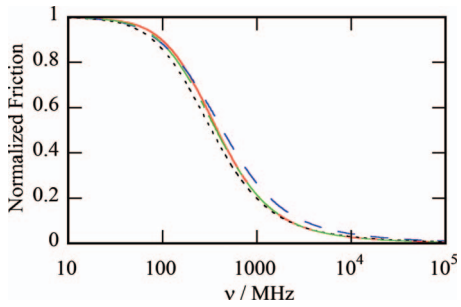

FIG. 6. The normalized friction spectra are compared with each other. The red solid, blue dashed, black dotted, and green dash-dotted curves denote $\tilde{\eta}(\nu)/\eta_0$, $\sigma_0/\sigma(\nu)$, $D_+/D_+(\nu)$, and $D_-/D_-(\nu)$, respectively.

We extend here the Nernst–Einstein relationship to the frequency-dependent one as follows. First, frequency-dependent diffusion coefficient of ion ζ is defined as

$$D_{\zeta}(\nu) \equiv \frac{1}{3} \int_0^{\infty} e^{-2\pi\nu t i} Z_{\zeta}(t) dt, \tag{33}$$

where $Z_{\zeta}(t)$ stands for the velocity autocorrelation function of ion ζ. Then the electric conductivity and the diffusion coefficients in Eq. (28) are replaced with the frequency-dependent ones as

$$\sigma_{\mathrm{NE}}(\nu) = \sum_{\zeta} \frac{\rho_{\zeta} z_{\zeta}^2 D_{\zeta}(\nu)}{k_B T}. \tag{34}$$

In Fig. 4, $\sigma_{\mathrm{NE}}(\nu)$ is plotted and compared with $\sigma(\nu)$. The peak frequency at several terahertzs is larger for the latter than for the former, and the collective mobility is smaller than the single-molecular one at the frequency above 10 GHz. In previous MD simulations, the damping and oscillation of the collective electric current correlation function are faster than those of the single-molecular velocity autocorrelation functions.[30,35,46] Since faster damping and oscillation correspond to the smaller mobility and the higher peak frequency, respectively, our theoretical result is consistent with these MD simulation results. The smaller mobility of the collective mode is then canceled by the weaker dispersion in the gigahertz region, and the Nernst–Einstein relationship for dc conductivity holds approximately. The ionicity close to unity is the result of the cancellation of the fast and slow dynamics, and it does not mean that the correlation between the diffusive motion of ions is weak.

Since both the self-diffusion coefficients and the electric conductivity are often discussed in terms of shear viscosity, it is interesting to compare the frequency dependence of these mobilities with the relaxation of shear viscosity shown in Fig. 1(b). Figure 6 exhibits $\tilde{\eta}(\nu)/\eta_0$, $\sigma_0/\sigma(\nu)$, $D_+/D_+(\nu)$, and $D_-/D_-(\nu)$ as the functions of frequency. Despite they are complex functions, only the real parts are plotted. The func-

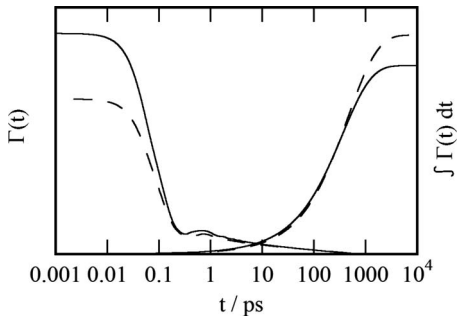

FIG. 7. The memory functions and their running integrals for the collective ($\Gamma_{el}(t)$, solid curves) and single-molecular ($\Gamma_s(t)$, dashed curves) modes are exhibited.

tions associated with mobility, $\sigma(\nu)$, $D_+(\nu)$, and $D_-(\nu)$, are inverted because mobility is inversely proportional to friction.

Comparing the shear relaxation and conductivity dispersion, it is found that the relaxation frequency of the former is smaller than that of the latter. These spectra of ionic liquid were measured experimentally at low temperature, and the faster relaxation of the electric conductivity was actually observed.[53] Our preliminary experimental result shows that such disagreement between the shear relaxation and electric conductivity dispersion also exists at room temperature.[34]

The difference between the shear relaxation and ionic mobility is usually attributed to the dynamic heterogeneity.[54,55] However, it is not the case of the present calculation because the relaxation of the self-diffusion is not faster than that of shear viscosity. The dispersion of the diffusion coefficient of anion follows the shear relaxation and that of cation is even *slower*. The electric conductivity is theoretically coupled to the shear viscosity through the self-diffusion of ions. The Stokes–Einstein relationship relates the self-diffusion coefficient to the shear viscosity, and the Nernst–Einstein relationship describes the electric conductivity in terms of the self-diffusion coefficients of ions. In our calculation, the decoupling between the shear viscosity and the electric conductivity dispersion is caused by the breakdown of the frequency-dependent Nernst–Einstein relationship, Eq. (34).

Figure 7 shows the memory function on the ionic current at $k=0$, denoted as $\Gamma_{el}(t)$, defined by

$$\Gamma_{el}(t) \equiv \frac{1}{\rho}\sum_{\alpha\gamma}\lambda_{\alpha\gamma}[\mathbf{J}^{-1}(k=0)\cdot\mathbf{K}(k=0,t)]_{\alpha\gamma}, \tag{35}$$

where $\lambda_{\alpha\gamma}=1$ when α and γ sites belong to the same species and $\lambda_{\alpha\gamma}=-1$ otherwise. The corresponding function for self-diffusion, given by

$$\Gamma_s(t) \equiv \sum_{\alpha\gamma}\lambda_{\alpha\gamma}[\mathbf{J}^{s,-1}(k=0)\cdot\mathbf{K}^s(k=0,t)]_{\alpha\gamma} \tag{36}$$

is also plotted for comparison. The memory functions $\Gamma_{el}(t)$ and $\Gamma_s(t)$ are so defined that they agree with each other when the random forces on different molecules are uncorrelated.

The collective memory function $\Gamma_{el}(t)$ is larger than $\Gamma_s(t)$ at $t<10$ ps which explains the lower mobility of the collective mode in the high frequency region. On the other hand,

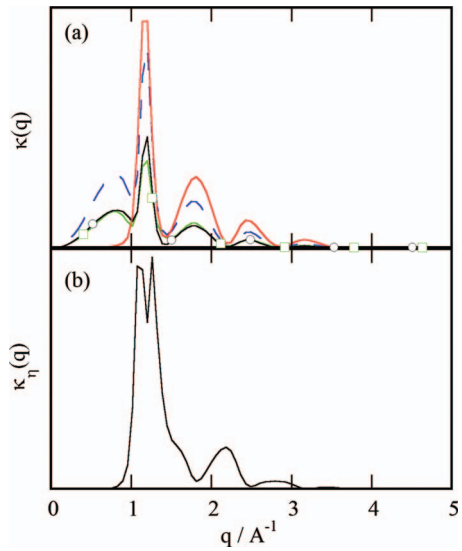

FIG. 8. The zero-frequency values of the memory functions are divided into the contributions of the liquid structures at various wavenumbers. In panel (a), the results on the memory functions on ionic currents are demonstrated. The meanings of the curves and symbols are the same as those in Fig. 2 except for the red solid curve that shows $\kappa_s(q)$. Panel (b) shows the wavenumber-resolved shear viscosity $\kappa_\eta(q)$.

the longer time tail is smaller for the collective mode, which is the reason for the weaker dispersion in the 100 MHz region and the dc electric conductivity larger than the prediction of Nernst–Einstein relationship.

According to the expression of the memory functions in the mode-coupling theory, Eqs. (13) and (14), the time-integrated values of $\Gamma_{el}(t)$ and $\Gamma_s(t)$ can be divided into the contributions of liquid structures at different wavevectors as

$$\int_0^\infty \Gamma_{el}(t)dt = \int_0^\infty \kappa_{el}(q)dq, \tag{37}$$

$$\int_0^\infty \Gamma_s(t)dt = \int_0^\infty \kappa_+(q)+\kappa_-(q)dq \equiv \int_0^\infty \kappa_s(q)dq, \tag{38}$$

$$\kappa_{el}(q) \equiv \frac{1}{6\pi^2}\sum_{\alpha\gamma}\lambda_{\alpha\gamma}\int_0^\infty dt\{q^2[\mathbf{c}(q)\cdot\mathbf{F}(q,t)\cdot\mathbf{c}(q)]_{\alpha\gamma}\mathbf{F}^{\alpha\gamma}(q,t) - q^2[\mathbf{c}(q)\cdot\mathbf{F}(q,t)]_{\alpha\gamma}[\mathbf{F}(q,t)\cdot\mathbf{c}(q)]_{\alpha\gamma}\}, \tag{39}$$

$$\kappa_\zeta(q) \equiv \frac{1}{6\pi^3}\sum_{\alpha,\gamma\in\zeta}\int_0^\infty dtq^2[\mathbf{c}(q)\cdot\mathbf{F}(q,t)\cdot\mathbf{c}(q)]_{\alpha\gamma}\mathbf{F}^{s,\alpha\gamma}(q,t). \tag{40}$$

The wavenumber-resolved frictions are plotted in Fig. 8(a). According to the resemblance of $\kappa_+(q)$ and $\kappa_-(q)$, the diffusive motions of cation and anion are coupled to the liquid structure in a similar way. On the other hand, the profile of $\kappa_{el}(q)$ is quite different from that of $\kappa_s(q)$ in that the effect of the structure of large wavenumber ($q>1$ Å^{-1}) is larger on the former than on the latter, which is canceled by the contribution at lower wavenumber.

The contribution of large-q liquid structure represents the short-range force such as collisional interaction. Since

the time scale of the collisional interaction is expected to be short, the larger contribution of the large-q region on $\kappa_{el}(q)$ is in harmony with the larger value of $\Gamma_{el}(t)$ in the short-time region as is shown in Fig. 7. Due to the strong electrostatic interaction between ions, an ion is likely surrounded by its counter ions. The repulsive collision thus occurs between a cation and an anion. In such a case, there is negative correlation between the forces on the cation and anion because of the action-reaction principle, which is the origin of the correlation that leads to the difference between $\Gamma_{el}(t)$ and $\Gamma_s(t)$ in the short-time region.

The smaller contribution of the small-q structure to the collective charge current than to the single-molecular modes has already been found in aqueous systems and molten salts by Yamaguchi and co-workers.[7,14] In their discussion, the small-q contribution to the collective charge current mainly originates in the electrostatic interaction, and it is described as the product of the fluctuations of charge- and number-density modes. Since number-density fluctuation is suppressed in dense liquids due to the small compressibility, the electrostatic friction on the collective charge current is also reduced compared with that on single-molecular modes. We consider that the same scenario holds on our present calculation on [mmim]Cl ionic liquid, and the small contribution of small-q structure is the reason for the weaker long-time tail of $\Gamma_{el}(t)$ than that of $\Gamma_s(t)$.

Although the decoupling between the frequency dependence of electric conductivity and ionic diffusivity seems to be explained by the difference in the liquid structure coupled to these modes, the situation is more complicated if shear viscosity is also taken into consideration. Shear viscosity is also divided into the contributions of different wavevectors according to Eq. (17) as

$$\eta_0 = \int_0^\infty \kappa_\eta(q) dq, \tag{41}$$

$$\kappa_\eta(q) \equiv \frac{k_B T}{60\pi^2} q^4 \int_0^\infty dt \, \mathrm{Tr}\left[\left\{\frac{d\mathbf{c}(q)}{dq} \cdot \mathbf{F}(q,t)\right\}^2\right], \tag{42}$$

which is plotted in Fig. 8(b). The zero-frequency shear viscosity comes almost exclusively from the high-wavenumber region ($q > 1$ Å^{-1}), as is the case of collective charge current. However, the relaxation frequency of the shear viscosity is close to those of the self-diffusion coefficients of ions, and the shear viscosity is decoupled from the electric conductivity, as is demonstrated in Fig. 6. Therefore, the relaxation time of the memory function is not determined solely by the wavenumber of the liquid structure, and we might need to analyze the contribution of each matrix elements of $\mathbf{F}(k,t)$.

Finally, we shall discuss on the large value of ionicity in both MD simulation and theoretical calculation. We consider at present that there can be two reasons as follows. The first one is that the electronic polarizability of ions are not considered in our model. In the case of MD simulation of inorganic simple molten salts such as KI, the inclusion of the electronic polarizability leads to the increase in the self-diffusion coefficients of ions with little effect on the electric conductivity, and the ionicity is thereby reduced.[56] The same scenario can also hold in the case of molecular ionic liquids.

The second possible reason is because the length of the alkyl chain of cation is short in our calculation. The experimental study indeed shows that the value of ionicity decreases with increasing the length of the alkyl chain.[51] The structure of room-temperature ionic liquids is considered to be inhomogeneous, consisting of polar and nonpolar domains. The heterogeneity increases with increasing the length of the alkyl chain of cation, and the inhomogeneous structure is experimentally confirmed by small angle x-ray scattering measurement when the chain length is sufficiently long.[57] The theoretical analysis shows that the number density fluctuation coupled to the memory function on the charge current is the fluctuation of the density mode weighted by the squared partial charges.[7,14] When the heterogeneous structure is present, the charge-square weighted number density fluctuation can be large even if the compressibility is small, which leads to the increase in the electrostatic friction on the charge current mode.

IV. SUMMARY

The mode-coupling theory for molecular liquid based on the interaction-site model is applied to a representative ionic liquid [mmim]Cl and the results are compared with MD simulation. Although the absolute values of the mobility are several times larger in the theoretical calculation than in the MD simulation, the theory describes the dynamics of the ionic liquid qualitatively well.

The theoretical dielectric relaxation spectrum shows a large relaxation in the 100 MHz region, as has been reported by microwave experiments for many ionic liquids. In addition, a resonance-shaped structure at several terahertzs, which was observed in a terahertz spectroscopic measurement, is also reproduced by the theory. The dielectric relaxation spectrum is divided into the contributions of translational and reorientational modes, and the theory shows that the dielectric relaxation is mainly ascribed to the translational mode. Although the dominance of the translational motion in the dielectric relaxation disagrees with the conventional assignment of dielectric relaxation experiments, it is in harmony with the mean-square displacements of ions whose slope is time-dependent in the time scale that is close to the dielectric relaxation time.

The large dispersion in the 100 MHz region is observed theoretically in all the transport properties studied here, that is, shear viscosity, self-diffusion coefficients, and electric conductivity. A detailed comparison of these dispersion spectra shows that the relaxation frequencies of shear viscosity and self-diffusion are close to each other, whereas that of electric conductivity is slightly higher than others. The higher relaxation frequency is related to the weaker tail in the memory function on the collective charge current, which is in turn attributed to the weaker coupling with the low-wavenumber liquid structure which represents the electrostatic friction.

In summary, the transport properties of the model ionic liquid are described by the mode-coupling theory qualita-

tively well, although the quantitative agreement is not so good. The theory enables us to analyze the molecular origin of the slow relaxation that is essential to understand the zero-frequency values of the transport coefficients. In a future plan, the theory can be applied to the solute-diffusion in ionic liquids, transport properties of the mixture of ionic liquid with water, carbon dioxide or lithium salts.

ACKNOWLEDGMENTS

This work is supported by the Research Grants from Mitsubishi Chemical Corporation Fund.

[1] H. Weingärtner, Angew. Chem., Int. Ed. **47**, 654 (2008).
[2] U. Balucani and M. Zoppi, *Dynamics of the Liquid State* (Clarendon, Oxford, 1994).
[3] J. P. Boon and S. Yip, *Molecular Hydrodynamics* (McGraw-Hill, New York, 1980).
[4] J.-P. Hansen and I. R. McDonald, *Theory of Simple Liquids*, 2nd ed. (Academic, London, 1990).
[5] S.-H. Chong and F. Hirata, Phys. Rev. E **58**, 6188 (1998).
[6] S.-H. Chong and W. Götze, Phys. Rev. E **65**, 041503 (2002).
[7] T. Yamaguchi, S.-H. Chong, and F. Hirata, J. Chem. Phys. **119**, 1021 (2003).
[8] T. Yamaguchi, T. Matsuoka, and S. Koda, J. Chem. Phys. **120**, 7590 (2004).
[9] T. Yamaguchi, T. Matsuoka, and S. Koda, Phys. Chem. Chem. Phys. **8**, 737 (2006).
[10] A. E. Kobryn, T. Yamaguchi, and F. Hirata, J. Chem. Phys. **122**, 184511 (2005).
[11] J. Bosse and M. Henel, Ber. Bunsenges. Phys. Chem. **95**, 1007 (1991).
[12] J. Bosse and Y. Kaneko, Phys. Rev. Lett. **74**, 4023 (1995).
[13] S. D. Wilke, H. C. Chen, and J. Bosse, Phys. Rev. E **60**, 3136 (1999).
[14] T. Yamaguchi, A. Nagao, T. Matsuoka, and S. Koda, J. Chem. Phys. **119**, 11306 (2003).
[15] C. G. Hanke, S. L. Price, and R. M. Lynden-Bell, Mol. Phys. **99**, 801 (2001).
[16] R. M. Lynden-Bell, N. A. Atamas, A. Vasilyuk, and C. G. Hanke, Mol. Phys. **100**, 3225 (2002).
[17] M. G. Del Pópolo, R. M. Lynden-Bell, and J. Kohanoff, J. Phys. Chem. B **109**, 5895 (2005).
[18] B. L. Bhargava and S. Balasubramanian, J. Chem. Phys. **123**, 144505 (2005).
[19] S. Bruzzone, M. Malvaldi, and C. Chiappe, Phys. Chem. Chem. Phys. **9**, 5576 (2007).
[20] S. Bruzzone, M. Malvaldi, and C. Chiappe, J. Chem. Phys. **129**, 074509 (2008).
[21] T.-M. Chang and L. X. Dang, J. Phys. Chem. A **113**, 2127 (2009).
[22] M. Malvaldi, S. Bruzzone, C. Chiappe, S. Gusarov, and A. Kovalenko, J. Phys. Chem. B **113**, 3536 (2009).
[23] S. Hayaki, K. Kido, D. Yokogawa, H. Sato, and S. Sakaki, J. Phys. Chem. B **113**, 8227 (2009).
[24] J. N. Canongia Lopes, J. Deschamps, and A. A. H. Pádua, J. Phys. Chem. B **108**, 2038 (2004).
[25] T. F. Miller III, M. Eleftheriou, P. Pattnaik, A. Ndirango, D. Newns, and G. J. Martyna, J. Chem. Phys. **116**, 8649 (2002).
[26] F. Hirata, *Molecular Theory of Solvation* (Kluwer, Dordrecht, 2003).
[27] M. P. Allen and D. J. Tildesley, *Computer Simulation of Liquids* (Oxford University Press, New York, 1987).
[28] S.-H. Chong and F. Hirata, Phys. Rev. E **57**, 1691 (1998).
[29] T. Yamaguchi and F. Hirata, J. Chem. Phys. **117**, 2216 (2002).
[30] C. Rey-Castro and L. F. Vega, J. Phys. Chem. B **110**, 14426 (2006).
[31] C. Schröder, C. Wakai, H. Weingärtner, and O. Steinhauser, J. Chem. Phys. **126**, 084511 (2007).
[32] W. Makino, R. Kishikawa, M. Mizoshiri, S. Takeda, and M. Yao, J. Chem. Phys. **129**, 104510 (2008).
[33] M. Fukuda, M. Terazima, and Y. Kimura, J. Chem. Phys. **128**, 114508 (2008).
[34] T. Yamaguchi, S. Miyake, and S. Koda (unpublished).
[35] M. G. Del Pópolo and G. A. Voth, J. Phys. Chem. B **108**, 1744 (2004).
[36] G.-E. Logotheti, J. Ramos, and I. G. Economou, J. Phys. Chem. B **113**, 7211 (2009).
[37] P. Mayer, K. Miyazaki, and D. R. Reichman, Phys. Rev. Lett. **97**, 095702 (2006).
[38] T. Yamaguchi, Y. Kimura, and N. Hirota, Mol. Phys. **94**, 527 (1998).
[39] C. Wakai, A. Oleinikova, M. Ott, and H. Weingärtner, J. Phys. Chem. B **109**, 17028 (2005).
[40] C. Daguenet, P. J. Dyson, I. Krossing, A. Oleinikova, J. Slattery, C. Wakai, and H. Weingärtner, J. Phys. Chem. B **110**, 12682 (2006).
[41] J. Hunger, A. Stoppa, S. Schrödle, G. Hefter, and R. Buchner, ChemPhysChem **10**, 723 (2009).
[42] J. Hunger, A. Stoppa, R. Buchner, and G. Hefter, J. Phys. Chem. B **113**, 9527 (2009).
[43] K. Yamamoto, M. Tani, and M. Hangyo, J. Phys. Chem. B **111**, 4854 (2007).
[44] E. I. Izgorodina, M. Forsyth, and D. R. MacFarlane, Phys. Chem. Chem. Phys. **11**, 2452 (2009).
[45] Y. Shim and H. J. Kim, J. Phys. Chem. B **112**, 11028 (2008).
[46] C. Schröder, M. Haberler, and O. Steinhauser, J. Chem. Phys. **128**, 134501 (2008).
[47] C. Schröder and O. Steinhauser, J. Chem. Phys. **131**, 114504 (2009).
[48] D. A. Turton, J. Hunger, A. Stoppa, G. Hefter, A. Thoman, M. Walther, R. Buchner, and K. Wynne, J. Am. Chem. Soc. **131**, 11140 (2009).
[49] A. Noda, K. Hayamizu, and M. Watanabe, J. Phys. Chem. B **105**, 4603 (2001).
[50] H. Tokuda, K. Hayamizu, K. Ishii, M. A. B. H. Susan, and M. Watanabe, J. Phys. Chem. B **108**, 16593 (2004).
[51] H. Tokuda, K. Hayamizu, K. Ishii, M. A. B. H. Susan, and M. Watanabe, J. Phys. Chem. B **109**, 6103 (2005).
[52] H. Tokuda, S. Tsuzuki, M. A. B. H. Susan, K. Hayamizu, and M. Watanabe, J. Phys. Chem. B **110**, 19563 (2006).
[53] A. Šantić, W. Wrobel, M. Mutke, R. D. Banhatti, and K. Funke, Phys. Chem. Chem. Phys. **11**, 5930 (2009).
[54] X. Xia and P. G. Wolynes, J. Phys. Chem. B **105**, 6570 (2001).
[55] V. Lubchenko, J. Chem. Phys. **126**, 174503 (2007).
[56] G. Jacucci, I. R. McDonald, and A. Rahman, Phys. Rev. A **13**, 1581 (1976).
[57] A. Triolo, O. Russina, H.-J. Bleif, and E. D. Cola, J. Phys. Chem. B **111**, 4641 (2007).